# Modelling secondary production in the Norwegian Sea with a fully coupled physical/primary production/individual-based *Calanus finmarchicus* model system

Solfrid Sætre Hjøllo[a, *], Geir Huse[a], Morten D. Skogen[a] & Webjørn Melle[a]

[a] Institute of Marine Research, Bergen, Norway

*: Corresponding author : Solfrid Sætre Hjøllo, email address : Solfrid.hjollo@imr.no

**Abstract:**

The copepod *Calanus finmarchicus* is the dominant species of the meso-zooplankton in the Norwegian Sea, and constitutes an important link between the phytoplankton and the higher trophic levels in the Norwegian Sea food chain. An individual-based model for *C. finmarchicus*, based on super-individuals and evolving traits for behaviour, stages, etc., is two-way coupled to the NORWegian ECOlogical Model system (NORWECOM). One year of modelled *C. finmarchicus* spatial distribution, production and biomass are found to represent observations reasonably well. High *C. finmarchicus* abundance is found along the Norwegian shelf-break in the early summer, while the overwintering population is found along the slope and in the deeper Norwegian Sea basins. The timing of the spring bloom is generally later than in the observations. Annual Norwegian Sea production is found to be 29 million tonnes of carbon and a production to biomass (P/B) ratio of 4.3 emerges. Sensitivity tests show that the modelling system is robust to initial values of behavioural traits and with regards to the number of super-individuals simulated given that this is above about 50,000 individuals. Experiments with the model system indicate that it provides a valuable tool for studies of ecosystem responses to causative forces such as prey density or overwintering population size. For example, introducing *C. finmarchicus* food limitations reduces the stock dramatically, but on the other hand, a reduced stock may rebuild in one year under normal conditions.

**Keywords:** *Calanus finmarchicus*, zooplankton, IBM, NORWECOM, end-to-end modelling, North-East Atlantic

# 1. Introduction

## 1.1. The life history of Calanus finmarchicus

The copepod *Calanus finmarchicus* (Gunnerus, 1765) is the dominant species of the mesozooplankton in the Norwegian Sea (Melle et al. 2004). The species is largely herbivorous and constitutes an important link between the phytoplankton and the higher trophic levels in the Norwegian Sea food chain (Aksnes and Blindheim 1996, Melle et al. 2004). The *C. finmarchicus* is vital to many of the planktivorous fish species including Norwegian spring spawning (NSS) herring (*Clupea harengus* Linneus, 1758), blue whiting (*Micromesistius poutassou*, Risso, 1826), and mackerel (*Scomber scombrus* Linneus, 1758 ), which feed in the Norwegian Sea during summer to utilize the abundant zooplankton resources (Dalpadado et al. 2000, Dommasnes et al. 2004, Broms and Melle 2007, Langøy et al. this issue). In addition to these migrating predators, there are large standing stocks of invertebrates and mesopelagic fish that feed on different stages of *C. finmarchicus* (Dalpadado et al. 1998, Skjoldal et al. 2004b). *C. finmarchicus* overwinter at depth mainly as copepodite stages 4 (C4) and 5 (C5), ascend towards the surface during early spring, mature, and produce eggs prior to and during the spring phytoplankton bloom (Marshall and Orr 1955, Niehoff et al. 1999, Broms and Melle 2007, Broms et al. 2009, Stenevik et al. 2009). The new generation stays in the upper waters and grows to stage C5. At this point, individuals may continue to mature and produce a new generation, or build up fat reserves and descend to overwintering (Hirche 1996a, Broms and Melle 2007, Broms et al. 2009).

Population dynamics of plankton results from net reproductive and advective rates (Aksnes and Blindheim 1996). The export losses from the Norwegian Sea population of *C. finmarchicus* into the Barents and North Seas provide very important input to these areas (Heath et al. 1999). Fish recruitment success in the Barents Sea is consequently positively correlated with inflow of warm *C. finmarchicus* rich water from the Norwegian Sea and coast (Sætersdal and Loeng 1987). In the North Sea, there has been substantial reduction in the abundance of *C. finmarchicus* during the recent decades (Planque and Fromentin 1996, Reid et al. 2003) that is partly attributed to a reduction in inflow from the Norwegian Sea (Heath et al. 1999) and partly due to change in species composition due to climate change. The low abundance of *C. finmarchicus* is a prime candidate for poor fish recruitment in the North Sea in recent years (Beaugrand et al. 2003, Nash and Dickey-Collas 2005, Payne et al. 2009), and *C. finmarchicus* is therefore a key species in many respects.

To organisms inhabiting the sea there are inherent problems in upholding life cycle closure due to the advective and diffusive forces that continuously act to disperse populations. While many marine fishes have solved this problem by counter current homing to distinct spawning areas, planktonic organisms face greater difficulties in maintaining life cycle closure. Instead planktonic species need to utilize the vertical and horizontal differentiation in the current pattern to close their life cycle. This is a particular problem in areas of strong advective regimes such as those bordering the Nordic Seas. Bryant et al. (1998) studied the drift pattern resulting from different vertical positioning that mimicked the vertical distribution of *C. finmarchicus*. They found that some areas of the Norwegian Sea such as the Norwegian Basin were able to retain particles over several years. Such retention is maintained by the seasonal vertical migration pattern with a northward flow during summer in the upper waters and compensatory southward flow in deep waters (>600 m) during winter. The model applied by Bryant et al. (1998) did not include growth, mortality, reproduction, and interannual variability in drift pattern. In order to fully understand the mechanisms

governing retention of *C. finmarchicus* in the core area in the Norwegian Sea it is important to include these factors.

## 1.2. Modeling spatial dynamics of plankton

There are two distinct methods for simulating the spatial dynamics of plankton, namely the Lagrangian (individual-based models (IBMs)) and Eularian approaches (e.g. Carlotti et al. 2000). Several models have been developed to simulate the spatial and population dynamics of *Calanus finmarchicus* both using 1D IBMs (Carlotti and Nival 1992, Carlotti et al. 1993, Carlotti and Radach 1996, Carlotti and Wolf 1998), 3D IBMs (Pedersen et al. 2001, Tittensor et al. 2003), and 3D Eularian (Speirs et al. 2005, Speirs et al. 2006) models. The different approaches have their pros and cons and in particular the Eularian models are numerically more efficient than IBMs, which on the other hand allow a more detailed biological description of individuals.
Another key element in IBM is the emphasis on mechanistic process formulation and emergent features in vital rates and traits (Huston et al. 1988, Huse et al. 2002, Grimm and Railsback 2005).

Huse (2005) presented a 1D IBM for *C. finmarchicus* based on evolving traits using a genetic algorithm under different predation levels. The results showed that the emergent life history traits were sensitive to the predation regime. This model was the core of the study by Samuelsen et al. (2009) which addressed the advection of *Calanus* from the Norwegian Sea onto the Norwegian shelf. This version of the model was 3D and coupled to the biogeochemical NORWECOM model. However the coupling was only one way so that the grazing by the *Calanus* was not taken into account in the model. Huse et al (in prep) developed the 1D *Calanus* IBM into a full 3D model and addressed the links between the adaptation of life history strategies and retention of *Calanus* in the Norwegian Sea basin. Skogen et al. (2007) ported the North Sea NORWECOM model to the Norwegian Sea and showed that the model reproduced the dynamics in the phytoplankton of the Norwegian Sea reasonable well. What has been lacking is a two-way coupling of *C. finmarchicus* and phytoplankton, taking into account the close interactions between plankton that is important for understanding the dynamics of the Norwegian Sea ecosystem (Skjoldal et al. 2004a).

The objectives of this paper are to simulate the *Calanus* distribution and production in the Norwegian Sea using a coupled 3D ocean/biochemical model with an embedded *C. finmarchicus* IBM taking into account growth, mortality, and reproduction as well as adaptive traits (Huse 2005), which control the interaction with the environment. The *C. finmarchicus* model relies on a) input from an ocean circulation model, which generates temperature, and turbulence and advection rates, and b) two-way interaction with a biogeochemical model which produces phytoplankton fields. Due to the relatively good data coverage of *Calanus* observations in 1997,we have chosen this year as the base year for our simulations. A one year long simulation is analyzed and compared to observations of chlorophyll-a and *C. finmarchicus* distribution and
production estimates for the Norwegian Sea. We thereafter perform experiments to study the effect of early/late diapause termination, food availability and initial stock size on the simulated *Calanus* production.

## 2. Methods

### 2.1. The ocean model component ROMS

The ocean model component is based on the Regional Ocean Modeling System (ROMS) version 2.1. ROMS is a three-dimensional baroclinic general ocean model, the development of which is described in a series of papers (Song and Haidvogel 1994, Haidvogel and Beckmann 1999, Haidvogel et al. 2000, Shchepetkin and McWilliams 2003, 2005). ROMS uses a topography-following coordinate system in the vertical that permits enhanced resolution near the surface and bottom (Song and Haidvogel 1994). Orthogonal curvilinear coordinates are used in the horizontal. A spline expansion has been used for vertical discretization which provides for an improved representation of the baroclinic pressure gradient (Shchepetkin and McWilliams 2003), vertical advection and vertical diffusion of momentum and tracers. Portions of the area of interest are ice-covered in parts of the years, and a thermodynamic sea ice module based upon an elastic-viscous-plastic (EVP) rheology after Hunke & Dukowicz (1997) and Hunke (2001) is included. The ice-ocean model system is run at high spatial resolution for a multi-year simulation and validated against available observations (Budgell 2005, Lien et al. 2006).

For the present study a model area that covers the North Atlantic from 20 degrees southand the Arctic was used. A stretched spherical coordinate grid (Bentsen et al. 1999) is used in the horizontal, with the "North Pole" situated in central Asia and the "South Pole" situated in the Pacific Ocean west of North America. In the Nordic Sea region, the horizontal resolution is approximately 20 km. There were 30 generalized σ-coordinate (s) levels, stretched to increase vertical resolution near the surface and bottom. No tides were included in the simulation, as the vertical mixing scheme employed was the LMD (Large and Gent 1999) parameterization, which has been found to produce good agreement with observed mixed-layer behavior in the deep ocean (Large and Gent 1999). The incoming and outgoing volume fluxes were both set to $1 \cdot 10^{-6}$ m3s-1, distributed uniformly across the two open boundary sections (outflow through the southern boundary and inflow through the Bering Strait). Zero normal gradients were specified for T and S, so that the only variations in these variables along the boundaries were due to atmosphericheat and salt (E-P) fluxes and vertical mixing. Zero normal gradients were also used at the open boundaries for all biochemical variables.

The atmospheric forcing was obtained from the NCEP/NCAR reanalysis data (Kalnay et al. 1996). Daily mean wind stress, and latent, sensible, downward short-wave radiative and net long wave radiative heat fluxes were applied as surface forcing after correcting for differences in model and NCEP surface conditions, such as in surface temperature and ice concentration. The flux corrections applied were developed by Bentsen and Drange (2000) and provide a feedback between the model surface temperature and applied heat fluxes, thus minimizing problems with drift in model surface temperatures. Precipitation was taken from the daily mean NCEP values. Snowfall was taken to be precipitation, corrected for snow density, when air temperature was less than 0°C. Evaporation was computed from the latent heat flux. River runoff was computed using the NCEP/NCAR Reanalysis daily accumulated surface runoff values over land that were routed to ocean discharge points using the Total Runoff Integrated Pathways (TRIP) approach of (Oki and Sud 1998). The data were modified for areas north of 60°N to account for permafrost hydrology and storage in snow cover.

To ensure that the ocean currents and hydrograpical structures within the study area

are sufficient covered and spun up, the model simulation was started from August 1, 1980, initialized from fields from a coarse resolution (50 km grid size) simulation of the North Atlantic and Arctic Oceans for the period 1948-2002 as described in Budgell (2005). A time step of 900 s was used for both the ocean internal mode and ice thermodynamic time step. A ratio of 30 was used between the ocean internal and external mode time steps, while a ratio of 60 was used between ice thermodynamic and dynamic time steps. We have used the full 3D velocity, hydrography and turbulence fields from the year 1997, i.e. ocean fields with a spin-up time of 17 years, as the environmental forcing for the coupled chemical/biological-*C .finmarchicus* model system.

## 2.2. The chemical-biological model

The chemical-biological model is coupled to the physical model through the hydrography and the horizontal and vertical movement of the water masses. The prognostic variables are dissolved inorganic nitrogen, phosphorous and silicate, two different types of phytoplankton (diatoms and flagellates), detritus (dead organic matter), diatom skeletals (biogenic silica), inorganic suspended particulate matter and oxygen. The processes included are primary production, respiration, algal death, remineralization of inorganic nutrients from dead organic matter, self-shading, turbidity, sedimentation, resuspension, sedimental burial and denitrification. In this two-way coupled version of the model system, the constant daily phytoplankton mortality of 10% day-1 is modified by using the geographically varying zooplankton grazing, as calculated by the *C. finmarchicus* model described later, with a low background mortality of 1% day-1 added. Sensitivity experiments show that the 1% day-1 background mortality has only minor impact on our results. Particulate matter has a sinking speed relative to the water and may accumulate on the bottom if the bottom stress is below a certain threshold value and likewise resuspension takes place if the bottom stress is above a limit. Remineralization takes place both in the water column and in the sediments. Parameterization of the biochemical processes and the exchange between the water column and sediment are taken from literature based on experiments in laboratories and mesocosms, or deduced from field measurements (Pohlmann and Puls 1994, Aksnes et al. 1995, Gehlen et al. 1995, Lohse et al. 1995, Mayer 1995, Lohse et al. 1996). The model is fully described in Skogen and Søiland (1998). The model has been coupled to the Princeton Ocean Model in the NORWegian ECOlogical Model system (NORWECOM) (Aksnes et al. 1995, Skogen et al. 1995, Skogen and Søiland 1998) and applied to study primary production, nutrient budgets and dispersion of particles such as fish larvae and pollution. This model system has been validated by comparison with field data in the North Sea/Skagerrak (Skogen et al. 1997, Søiland and Skogen 2000, Skogen et al. 2004). Recently, the chemical model has been coupled to ROMS to study Norwegian Sea primary production (Skogen et al. 2007).

The biochemical model was run in off-line mode for the year 1997 using 3 days mean physical fields from the ROMS simulation described above. The time-step was 1 hour. The incident irradiation used in the biochemical model is modeled using a formulation based on Skartveit & Olseth (1986, 1987, EMEP/MSC-W 1998) using data for global daily downward short-wave radiation from the NCEP/NCAR reanalysis data set. The nutrient fields are initialized January 1 using typical values for winter nutrients of Atlantic Water in the Norwegian Sea, 12.0, 5.5 and 0.8 µM of inorganic nitrogen, silicate and phosphorous respectively (F.Rey, unpublished data), which are believed to be representative for the year 1997 since the annual variations in winter nutrient concentration are no greater than about 10% (Rey 2004). The model is initialized with some small amounts of algae (0.10mgNm-3) for both diatoms and flagellates. Inorganic nitrogen is added to the system from the atmosphere (200

mgN/m2/year) (EMEP/MSC-W 1998), while there are no river nutrients, as they are mostly affecting near coastal waters and not our open ocean focus area.

## 2.3. The Calanus finmarchicus individual based model

The 3D *Calanus finmarchicus* individual based model takes into account growth, mortality, movement and reproduction of *C. finmarchicus* as well as adaptive traits (Huse 2005), which control the interaction with the environment. The model addresses the entire life cycle of *C. finmarchicus*, and the main life history features and vertical movement are emergent properties resulting from many generations of evolution using a genetic algorithm. The purpose of the model is to evolve behavioral and life history strategies of *C. finmarchicus* using a genetic algorithm, a physiological model, and a detailed description of the environment in order to understand the *C. finmarchicus'* behavioral and life history strategies and their effect on population dynamics and retention. The *C. finmarchicus* IBM has been described in previous studies (Huse 2005, Samuelsen et al. 2009) and for more details on the exact representation of the details see Huse et al (in prep).

*State variables.* The model comprises individuals and their environment. The attribute vector (Chambers 1993) of super-individuals consists of different states including their stage, internal number (number of *Calanus finmarchicus* individuals represented by the super-individual), weight, fat level, age, depth etc (Table 1). The strategy vector (Huse et al. 1999), which is evolved, contains all the life history and behavioural strategies of individuals and comprises six behavioural and life history traits. The life history traits include the date for ascent from overwintering to the surface (WUD), the day for initiating fat allocation (AFD) in copepodite stage 5 (C5), fat/soma ratio needed before descending to overwintering (FSR), overwintering depth (OWD), and two genes (VM1 and VM2) that determine the day time depth of copepodites outside of overwintering area. The three former traits were introduced by Fiksen (2000). Even though the individual-based structure is appealing, it is impossible to simulate copepod population dynamics on a truly individual basis due to the great abundances involved, and *C. finmarchicus* is therefore simulated using the super-individual approach (Scheffer et al. 1995). A super-individual represents many (~1012) identical individuals and the number of such identical siblings is an attribute of the super-individual. Each super-individual is given a certain influence area, defined as a function of total number of super-individuals at the start of a simulation.

**Processes overview and scheduling.** The processes governing the individuals are growth, mortality, movement and reproduction. *Calanus finmarchicus* has 13 different stages including an egg stage, six nauplia stages, five copepodite stages and an adult stage (including both males and females). *C. finmarchicus* does not commence feeding until the third nauplia stage (N3), and for stages below this, stage longevity was calculated as a function of temperature (Carlotti and Wolf 1998). For stages N3 and above, growth is calculated as a function of phytoplankton density, temperature and size using a bioenergetics model (Carlotti and Wolf 1998). The *C. finmarchicus* is assumed to change stage when a stage-specific critical weight (Carlotti and Wolf 1998) is achieved. The critical weights are constant in time and place, and do thus not take into account environmental effect on the critical weights (Gentleman et al. 2008). This will be a subject for future model refinement. For the egg and nauplia stages, mortality consists of unspecified causes (taken from Ohman et al. 2004) and tactile predation. For the copepodite and adult stages, mortality is parameterized separately for the following causes: fish predation (geographically uniform, daylight & prey size dependent and restricted to upper 600m), invertebrate predation (geographically uniform and day/night varying, exponentially decaying in upper

1000m), starvation (stage dependent weight limited), stage dependent ackground mortality, reproduction stress (individuals who has reproduced more than > 800 eggs are removed) and export (transported across the Greenland Scotland ridge, into the Labrador Sea or reaching the artificial boundary at 62°N). Also, slightly increased autumn mortality for light individuals not in overwintering stage is added. For individuals in diapause, no vertical movement is calculated, but for other individuals, movement is calculated either as a function turbulence and sinking (stages < N3) or by adapted rules. A sex ratio of 50% is assumed, and males are removed from the population after one spawning event, as male *C. finmarchicus* have only a brief functioning after which they are expendable (Hirche 1996b). Fat is allocated to structural growth for immature individuals, but mature individuals and C5s preparing for overwintering allocate their surplus energy into fat storage. During times of negative growth, the stored fat is depleted before the structural weight is reduced.

***Reproduction.*** Adults can reproduce when their structural weight is above 90 µg, they have attained enough fat reserves to spawn a batch of eggs, and they are positioned within the upper mixed layer (<40 m). If these criteria are fulfilled new super-individuals are produced. An offspring inherits the strategy vector from its parent, but random changes take place with a probability of 0.06 per trait or weight on the strategy vector. Such mutations take place by changing the values randomly by ±20% of the value. The internal number of the new superindividual is a function of the batch size and the internal number of the parent individual. New super-individuals are initiated as eggs at the same depth as the parent. Following reproduction the weight reserve of the parent super-individual is reduced by an amount corresponding to the clutch size multiplied by the egg weight.

***Flows between submodels.*** The models are linked so that the IBM receives input on phytoplankton density. The *Calanus* individuals then feed on the phytoplankton, a grazing rate is calculated, and the new phytoplankton biomass is calculated and updated in the NORWECOM model. The *Calanus* feed simultaneously in order to avoid any consistent differences in food provisioning among individuals. This is done by first adding up the total demand for food, and then adjust the available resources so that all IBMs get the same fraction of food based on their demand and what is available. Initial test simulations with one way coupling of NORWECOM and Calanus models showed that the grazing rate very seldom exceeded 20% day, and this rate has been used as a threshold on grazing to avoid a too fast removal of phytoplankton in grid cells.

***Initiation:*** At start of simulation, the overwintering population of *Calanus finmarchicus* is distributed in the deeper Norwegian Sea basins. This distribution mimic overwintering population in Arctic Intermediate Water, which is a habitat suitable for overwintering by conserving energy, avoid predators and survive until reproduction can be accomplished (Dale et al. 1999, Skjoldal et al. 2004b). The initial field is found by first seeding the area uniformly with *C. finmarchicus*, and then run the model with repeated physical forcing until a non-evolving overwintering field appears. Such a steady-state is found after 4 years of simulation.

Simulations with the fully coupled ocean-biogeochemical-*Calanus finmarchicus* model system The simulations are organized in two parts: first, we perform a reference run which is analyzed and validated towards available observations, and then we experiment with the *Calanus* life cycle, food availability and population size and discuss their effect on *Calanus finmarchicus* quantities as biomass, abundance, distribution and production. The simulations are summarized in Table 2.

## 2.4. Experiment REFRUN: The reference run

The setup is as described in Section 0- 0; i.e. with physical forcing for the year 1997 and for a domain covering the North Atlantic and the Arctic, while the *Calanus finmarchicus* population is modeled for the Nordic Seas (the area depicted in figure 1 plus the Barents Sea). Initially a biomass of 8.7 mill tonnes carbon (C) C5 *C. finmarchicus* individuals in diapause and at a mean overwintering depth of 443m is found. The initial overwintering field is produced through a 4 year long adjustment process (Sec 2.3), and represents the general knowledge and non-evolving model field of size and geographical distribution of the overwintering population, rather than being specific for 1997. Strategy vectors are based on an earlier version of the evolving traits in Huse et al (in prep). Diapause termination, i.e. wake-up-day (WUD), is at February 10 plus a random number of days within the next 2 months. Allocation-to-fat-day (AFD) is defined as a random number of days within the interval 30-90 after wake-up-day. An artificial boundary is placed at 62°N, causing *C. finmarchicus* individuals south of this boundary not to survive, but they are still included in the mass balance calculations.

## 2.5. Experiments varying the Calanus life cycle, food availability or population size

Experiments WUDLATE,WUDEARLY,WUDLIGHT: Varying the diapause termination

To study the effect of the timing of the springtime start of *Calanus finmarchicus* evolution on the total production and biomass distribution, we have performed two tests with the WUD start day being 10 days earlier (Jan 30; WUDEARLY) or later (Feb 20; WUDLATE), which provide a reasonable time window. Based on weekly observations at OWSM (Figure 5), the *C. finmarchicus* evolution starts in first part of March, and we have performed one test (WUDLIGHT) with day light dependent WUD, i.e. that WUD is chosen as the day with same amount of daylight as at March 1 at Ocean Weather Ship M (66°N, 2°E). This corresponds to WUD varying between Feb 24 in south and March 10 in northern areas, without a random number of days added; thus all the *C. finmarchicus* at certain latitude start ascending at the same day. Note that AFD is dependent on WUD and will change accordingly. Other parameter settings as in the reference run.

## 2.6. Experiment NOFLA: Effects of changed food availability

In the primary production model, both diatoms and flagellates are produced and are available food for *Calanus finmarchicus*. Flagellate mass may be interpreted as both flagellates and other microzooplankton available as food for *C. finmarchicus* in nature. However, to simulate the *C. finmarchicus* diet switch to diatoms, we have performed a simulation where *C. finmarchicus* have access to diatoms only, and flagellates have increased background mortality (10%). Other parameter settings as in the reference run.

## 2.7. Experiment LOWINI: Low biomass in the overwintering population

The interannual variation in springtime Norwegian Sea zooplankton biomass is large, and in 2008 the biomass is at the lowest recorded since 1997; 7.1 g/m2, in contrast to 14.2 g/m2 in year 2000. (Ellertsen and Melle 2009). We have performed one simulation with initial *Calanus finmarchicus* biomass reduced by 50%, but distributed among 50.000 super-individuals initially as in the reference run. This experiment

represents a situation with geographical *C. finmarchicus* distribution as in the reference run, but with lower biomass and abundance. Other parameter settings as in the reference run.

Observations of Calanus finmarchicus abundance and zooplankton biomass
for model validation Data used for model validation are net samples obtained within the Nordic Seas, during the year 1997, at Weather Station Mike and during regional surveys (Figure 1). The net samples used here are vertical and oblique samples of the upper 200 m with WPII 180 μm mesh size. The samples were obtained during all seasons. Biomass samples are produced by sieving net catches through 2000, 1000 and 180 μm meshes, rinsing with fresh water, drying and weighing.

Abundance data are from sorting and counting of formalin samples under the microscope. All data are from Institute of Marine Research monitoring and research programs and contained at the institute's databases. For more details on methods, we refer to Broms et al. (2009).

# 3. Results

We start by describing the creation of the initial field, then look more closely at the reference run, perform a model validation and thereafter proceed to describe the effect on key variables of changing wake-up-day, food availability and initial mass.

## 3.1. Creating the initial field

The initial field is found by first seeding the area uniformly with 17 mill tonnes C *Calanus finmarchicus* distributed on 50.000 super-individuals, and then run the model with repeated physical forcing until a non-evolving overwintering field appears. We monitored the integrated biomass, production and abundance, number of super-individuals and geographical distribution of abundance (Figure 2), and found that after 3-4 years, geographical distribution and the integrated quantities were only minor varying and a non-evolving field achieved. However, the number of super-individuals increased by ~50.000 super-individuals every year, and this is computationally inefficient. From the overwintering field at year 4, we therefore combined super- individuals within adjacent or same grid cell and with approximately equal (within 50%, 20% or 5%) fat content and structural weight, reducing the number of super-individuals to 120.000, 47.000 or 23.000. We ran the model 1 year with identical settings and initial fields, but using the varying number of super-individuals. Comparing integrated biomass, production and number of individuals as well as and geographical distribution of abundance in these experiments (Figure 3), we see that there are only minor spatial differences between 23.000/47.000/120.000 and the original field with 200.000 super-individuals, but the time series show that the number of super-individuals in the initial field cannot be reduced to ~23.000 without introducing model setup effects on biomass, production or number of individuals.

Thus, as initial field used in all simulations we use 47.000 overwintering C5 individuals from the lower left abundance panel in figure 3.

The reference run The reference run was initiated with the initial field evolved through the 4 year spinup phase, encompassing 8.7 mill tonnes C of *Calanus finmarchicus* biomass distributed on $1.8 \cdot 10^{17}$ individuals/47.000 super-individuals (Figure 4). The biomass experiences first a vigorous reduction (4, left panels), before mid-April, when the new generation starts growing and the biomass increases and

reaches its maximum late summer. The biomass at the end of simulation is 8.0 mil tonnes C, slightly lower than at start. Production starts in April and reaches its maximum (0.3 mill tonnes C per day) in July. The number of individuals in the simulation decreases for 2-3 months, and then rapidly grows from the initial number of overwintering C5 individuals of ~1.8·1017 to 7·1017. At the end of the year, almost the same number as initially of overwintering C5 are found (1.7·1017). The large variability in number of individuals through the year is reflected in the number of super-individuals, which due to reproduction are close to doubled during one year of simulation. Snapshots of the winter abundance (Figure 4, right panels) show highest values in the western Norwegian Sea and along the Norwegian continental slope (~200.000 individuals/m2). In May, the highest abundance is found south of Iceland and along the Norwegian Coast and up towards West-Spitsbergen, and more than 300.000 individuals pr m2, and peak values of ~40.000 no/m2 of C6 individuals, can be found. The distribution at the end of year is close to the initial field distribution, i.e. the overwintering population of *C. finmarchicus* is found in the deeper part of the Norwegian Sea and around Iceland, along the western part of Spitsbergen. The abundance here is on average ~100.000 no/m2, but clusters with higher abundance can be found along the Norwegian continental slope.

### 3.2. Model validation

Unevenly distributed observations in time and space complicates model - data comparison, but here we perform several types of model validation: first by comparing observations and modeled zooplankton and chlorophyll-a concentration in a well-sampled point (Ocean Weather Ship M at 66°N, 2°E), and then by comparing modeled and observed abundance and biomass at 20 several positions across the Norwegian Sea. Distributions and derived variables will also be compared to values from literature when available. Observations from a station in the inflowing Atlantic water in the southern Norwegian Sea
(Ocean weather Ship M (OWSM), Figure 5a) shows that the first *Calanus finmarchicus* individuals (overwintering C4, C5 and C6) appear in February, and in April, a new generation is produced and there is a rapid growth and evolution of the population through the stages C1-C5. The number of individuals/m2 varies between 0 and 50.000, with the highest numbers being C4 copepods. The simulated *C. finmarchicus* distribution show the first C5 and C6 individuals appearing in January, somewhat earlier than in the observations, and then approximately two month later reproduction has started and C1-C6 copepods are found. As the 95% confidence intervals show, the variability is large both in observations and predictions, but generally the modeled abundance is above observed abundance for the stages C1-C4, while for C5 and C6 the model resembles the observed peak levels. The successive evolution through the different stages reported by Hirche et al.(2001) are seen both in the observations in Figure 5 (noting that both C4 and C5 is part of the overwintering population) and in the model, although is more widespread in time in the model. The predicted C5 abundance in spring is at an elevated level compared to the observations, but is at same level in July, when C5 descends to their overwintering depth. In late summer/autumn, the predicted C5 abundance is very high, indicating late descend to overwintering or advective processes. Observed chlorophyll-a (Chl-*a*) integrated in upper 50m at OWSM (Figure 5b) shows a first peak around day 90, before the maximum peak of 190 mg/m2 is found at day no 140 (mid-May). The chlorophyll levels remains elevated for the rest of the year, before retreating in winter. The modeled Chl-*a* shows a first peak in late March, matching the observations, and then a second peak in end of May, 2 weeks later than seen in the observations.

The chlorophyll level remains lower than the observations for the rest of the year.

Also plotted in Figure 5b) is Chl-*a* from Skogen et al (2007) who used the same set-up of ROMS/NORWECOM, but with a constant zooplankton grazing rate (10% day-1). Skogen et al (2007) found the mean annual production in the Norwegian Sea and day of peak of Chl-*a* at OWSM to be in accordance with the observations, although the variability of day of peak Chl-*a* was lower than in the observations (2 vs 6 weeks for the period 1981-2004). With the inclusion of the *C. finmarchicus* IBM the first phytoplankton bloom appears ~10 days earlier at OWSM than in the old version, in better accordance with observations (Rey, 2004), while the day of peak Chl-a is found 15 days later in the present study.

### 3.3. Abundance

A composite picture of observations of *Calanus finmarchicus* abundance 1993-1997 [Fig 6.13, Melle et al (2004)], show patches of more than 600.000 and 50.000 no/m2 for C1-C6 and C6 respectively, distributed all over the Norwegian Sea as far west as to an assumed Iceland- Spitsbergen line. The predicted abundance (Figure 4, right panels) shows the same patchy distribution, although with somewhat lower maximum number of individuals in the patches. Figure 6, upper panel, show C1-C6 abundance predicted and from observations at several locations through the year 1997, grouped into monthly means. Abundance increases from April and reaches its maximum level in May both in observations and model, but the model abundance is higher, although still within the confidence limits. The elevated model abundance sustains until late autumn, and is from June an onwards significantly higher.

### Biomass

Figure 6, lower panel, show biomass predicted and estimated from observations [estimated assuming 50% & 70% *Calanus* (predominantly *C. finmarchicus)* content in the size classes <1000µm and 1000-2000µm, as suggested by Skjoldal et al (2004a)]. Observed and modeled biomass follows each other until June, and both model and observations has maximum values ~4-5 g/m2, but the model maximum are found 1 month later than in the observations. Modeled autumn biomass is lower than observed biomass. Integrated Norwegian Sea quantities

In the upper 200m the summer *Calanus* biomass is estimated to 48.3 mill tonnes wetweight by Skjoldal et al (2004a), assuming 50% - 70% - 30% *Calanus* content in the size classes<1000µm,1000-2000µm, >2000µm. Using a PB-ratio of 6, their estimated *Calanus*(predominantly *C. finmarchicus)* production is 290 mill tonnes. From our model simulation,(Figures 4 and 5), an annual production of 29*6.67=193 mill tonnes and mean top to bottombiomass in summer (May-July, when most of the super-individuals are found above 200m) of6.7*6.67=45 mill tonnes are found. In the model, biomass is measured in carbon weight, but forcomparison with the wet weight values found in literature, we use a convert factor of 6.67,following Hirche et al (2001)and Ashjian et al.(2003). The predicted biomass and production arethus comparable to observed estimates, although care should be taken in this comparison sincethe model estimates are for the total model area and all depths. PB-ratio in the model is found tobe 4.3, i.e. lower than the values used by Skjoldal et al (2004a). As a curiosity, we note that theproduction estimate by Skjoldal et al (2004a) of 290 mill tonnes would be reduced to 208 milltonnes using the PB-ratio found in our simulations.Experiments varying the Calanus life cycle, food availability or populationsize

WUDLATE, WUDEARLY and WUDLIGHT experimentsThe effect of varying the wake-up-day on biomass and production is shown in Figure 7. In thespring, 10 days later WUD produces higher biomass but the production is as in the reference run, indicating lower mortality. The biomass stays elevated, and at end of the year it is

10% above thereference biomass. Annual production is increased by 12%. Early or light dependent wake-updayreduces biomass by 20% or 40%, and production is reduced all year long, resulting in 20%or 50% reduced annual production. We note here that even with a minimum biomass of 0.2milltonnes in April, as in the WUDLIGHT experiment, rebuilding of the stock is possible.

Unlike other studies (Samuelsen et al. 2009, Huse et al. in prep), our model systems has two-way coupling between the phyto- and zooplankton fields, which allows exploration of top down/bottom-up control links. From a 10 year long simulation with ROMS/NORWECOM with constant zooplankton grazing rate, Skogen et al. (2007) found the mean annual primary production in the Norwegian Sea and day of peak of Chl-*a* at OWSM to be in accordance with the observations, although day of peak Chl-*a* variability was lower than in the observations (2 vs6 weeks for the period 1981-2004). For over-wintering *C. finmarchicus*, starvation was found tobe the second most important mortality cause in the model, and this may be due to mismatch between phytoplankton bloom and start of *C. finmarchicus* annual life cycle. Our experiments with varying wake-up-day and corresponding time displacement of grazing rate on phytoplankton show that the effect of wake-up-day of *C. finmarchicus* is larger on production than on the annual biomass; i.e. late zooplankton blooms are compensated by production indifferent areas (the deeper Norwegian basins) and/or a more efficient transfer of energy from phytoplankton to zooplankton, and thus the consequences of phyto/zooplankton bloom mismatch may be reduced.

### 3.4. Effects of changed food availability or initial stock size

In experiment NOFLA, we have studied the effect of food availability by letting *Calanusfinmarchicus* have access to diatoms only. This has a dramatic effect on the number ofindividuals and thus the biomass (figure 7), which is reduced from 8 million tonnes C in the startpopulation to <2 million tonnes in August, when the simulation was ended. The overwintering *C.finmarchicus* are not allowed to produce a sufficient number of eggs due to low fat and structural weight.

The effect of starting the simulation with reduced initial mass (but same amount of *C. finmarchicus* individuals) is also shown in Figure 7, and despite much lower *C. finmarchicus* abundance in spring, the biomass is increasing in April as in the reference run, and at the end of the year the standing stock is of ~6 mill tonnes C, which is a 50% increase and only 20% less than in the reference run. This means that a relatively small overwintering stock can produce a good year-class if food is available. We saw the same in the WUDLIGHT run, where the minimum biomass in April was even lower than in LOWINIBIO.

### 3.5. Strategy vector changes

The strategy vector encompasses the wake-up-day and allocation-to-fat-day, and these vary between each super-individual. Since offspring inherits their parent's strategies, a population with changing strategies can arise, and that need to be taken into account when performing multiyear- simulations. By monitoring the population's daily mean values of WUD and AFD in the different experiments, we can identify experiments which changing strategies. We found that for all these 1 year long simulations (Figure 8), the mean WUD is only minor changed (2-4 days) through the year. All experiments except WUDLIGHT have later mean WUD at end of year than at start. The change in mean AFD is larger, ~10 days. This is due to the model artifact that superindividuals with high AFD number have a greater chance for reaching sufficient fat content and structural weight to reproduce, and a population with higher AFD arises.

## 4. Discussion

We have presented a fully coupled 3D model system that integrates a Eularian biogeochemical model with an individual based model for *Calanus finmarchicus* dynamics at basin scale. This is a novel modeling concept that allows studies of *C. finmarchicus* life history features and population dynamics while at the same time having fully coupled trophic links. There is presently a lot of interest in developing end to end models of marine ecosystems that integrate the physical forcing with all the major trophic levels represented (Travers et al. 2007, Cury et al 2008, Rose et al. 2010, Huse and Fiksen 2010). The coupled model presented here has been extended to include three planktivorous fish stocks namely herring, mackerel and blue whiting (Utne et al, this issue) using the same individual-based representation as for *C. finmarchicus*. A notable difference between the fish and *Calanus* models is active horizontal migration module included in the fish model. This illustrates the great flexibility in approach and its potential advantage in adding on the higher trophic levels and achieving true end to end models.

A fundamental question of interest is whether our model resembles the real world, here represented by observations, and we therefore performed a model-observation comparison of single stations and integrated values. Comparisons of predictions and observations show that the model values are on the high side for abundance and low side for biomass. The high-frequent observations at OWSM show that the model overestimating of small copepodites (C1-C4) is larger than for C5 and C6. The mismatch between observations and model may have several explanations, and some of them can be: a) Model weakness, for example in the mortality formulation, or model timing: the analysis of OWSM showed that the model had an earlier start of *C. finmarchicus* bloom in springtime, and since wake-up-day influence population development (see Section 0), a day-to-day comparison of model and observations are difficult, b) observational challenges:

i)      stage longevity is very short for the smallest copepods (~a few days for C1-C3), and there will thus be high day-to-day variability in observed abundance,

ii)     undersampling; i.e. WP2-nets with 200µm mesh size under-samples copepods <500µm (Munk et al. 2003), but the degree of undersampling with 180µm mesh size is unknown,

iii)    methodological uncertainties: *C. finmarchicus* content in the size classes are watermass-, areaand time dependent (Broms and Melle 2007), and the use of the constant 50/70% content may lead to too low modeled biomass estimates especially in spring and autumn.

We also note that there are large interannual variations in biomass in this area (Skjoldal et al. 2004b), and as the initial biomass field of the model is not specific for the year 1997, discrepancies was expected. In fact, 1997 where a year with late spring stabilization and very low production in the Norwegian Sea (Rey 2004, Ellertsen and Melle 2009), and may thus not be representative.

The importance of the ocean physics for the *Calanus* modeling will be further explored in forthcoming studies, but we note here that our ocean model resolution of 20km is eddy permitting, but not resolving the Rossby radius (~5-10km in the Norwegian Sea) and is thus not eddy resolving. The limited ocean resolution restrict

the on/off shore shelf transport of *C. finmarchicus* (Samuelsen et al. 2009), underestimates the primary production at the Norwegian shelf (Hansen and Samuelsen 2009) and probably also in the open ocean area (Falkowski et al. 1991), and also reduces generation of mesoscale eddies, which are productive habitats for higher trophic levels (Godø et al. In prep). When estimating production from biomass, a choice of PB-ratio has to be taken. Our model complex allows the determination of the PB-ratio as an emergent parameter, which can be useful when estimating annual production based on biomass from only selected months. For example, using May biomass only (Figure 4), our model complex would suggest using a PB-ratio above 7, while using June or July biomass estimates, a lower PB-ratio would be appropriate. Observations show that total biomass of the Norwegian Sea ecosystem is ~210 million tonnes, of which meso- and macrozooplankton make up more than 70%, and *Calanus* alone constitute about one quarter (Skjoldal et al. 2004a). Pelagic and mesopelagic fish represent ~12% of the Norwegian Sea biomass, and consume about 1/3 of the production of *Calanus*. In the model, mortality is parameterized separately for the following causes: fish predation (geographically uniform, daylight & prey size dependent and restricted to upper 600m), invertebrate predation (geographically uniform and day/night varying, exponentially decaying in upper 1000m), starvation (stage dependent weight limited), stage dependent background mortality, reproduction stress (individuals who has reproduced more than > 800 eggs are assumed to be exhausted and removed from the population (Carlotti and Wolf 1998) and export (transported across the Greenland Scotland ridge, into the Labrador Sea or reaching the artificial boundary at 62°N). Fish predation causes ~40% of the biomass loss and is the primary mortality cause for *C. finmarchicus* copepods. A natural extension of our model system is to include observational based fish predation by adding IBM sub models with annual migration patterns for herring, mackerel and blue whiting (Utne et al. this issue), as well as to include other meso/macrozooplankton sub models.

## 5. Conclusions

By coupling a well-documented ocean model to a two-way coupled primary-production / IBM *Calanus finmarchicus* model system, we have developed a model system able to describe the dynamics within the *C. finmarchicus* population in the Norwegian Sea itself, as well as the coupling between the *C. finmarchicus* and the physical-biological surroundings. One year of development of the *C. finmarchicus* population is analyzed and compared to observations where available, and we found the model system to capture the main features of the Norwegian Sea *C. finmarchicus* dynamics. We used *C. finmarchicus* observations from 1997, the year mimicked in the physical forcing, although the initial *C. finmarchicus* field is not year specific. High *C. finmarchicus* abundance is found along the Norwegian shelf-break in the early summer, while the overwintering population is found along the slope and in the deeper Norwegian Sea basins.

The timing of the spring bloom is generally later than in the observations. Annual Norwegian Sea production is found to be 29 mill tonnes C (~193 mill tonnes wet weight), which is lower than estimates from observations (290 mill tonnes; using summer biomass of 48 mill tonnes wetweight and assuming a PB-ratio of 6). Sensitivity experiments show that initial biomass distributed on 50.000 super-individuals is sufficient, and that the modeled life cycle strategies changes are limited. Food access is of importance; for example, limited phytoplankton mass may reduce the stock in one year. On the other hand, the model predicted that a strongly reduced *C. finmarchicus* stock at start of year may almost fully recover during one

year, if food is available. Late *C. finmarchicus* ascent in spring produces 10% increased mean annual biomass, while annual production is increased by 20%. Early or light dependent wake-up-day, reduced food access or low initial biomass all lead to lower production and biomass than in the reference run. In 2011, the world's first commercial offshore fishery on *C. finmarchicus* opened in the Norwegian Sea, which motivates further work in estimating the regional production of this stock. Despite its complexness and weaknesses, a two-way coupled model system allows more realistically quantification of the zooplankton variability in time and space, which is important for understanding variation in fish recruitment, for example. It also opens the possibility to further explore the interaction between the lower trophic levels and the environments, as well as being a tool for studying effects of future changes in the forcing fields, both with regards to climatic and ecological changes.


# Acknowledgements

# References

Aksnes DL, Blindheim J. 1996. Circulation patterns in the North Atlantic and possible impact on population dynamics of *Calanus finmarchicus*. Ophelia 44:7-28.

Aksnes DL, Ulvestad KB, Baliño BM, Berntsen J, Egge JK, Svendsen E. 1995. Ecological modelling in coastal waters: Towards predictive physical-chemical-biological simulation models. Ophelia 41:5-36.

Ashjian CJ, Campbell RG, Welch HE, Butler M, Van Keuren D. 2003. Annual cycle in abundance, distribution, and size in relation to hydrography of important copepod species in the western Arctic Ocean. Deep Sea Research Part I: Oceanographic Research Papers 50:1235-1261.

Beaugrand G, Brander KM, Lindley JA, Souissi S, Reid PC. 2003. Plankton effect on cod recruitment in the North Sea. Nature 426:661-664.

Bentsen M, Drange H. 2000. Parameterizing surface fluxes in ocean models using the NCEP/NCAR reanalysis data. RegClim General Technical Report 4. Norwegian Institute for Air Research, Norway. Pp:44-57.

Bentsen M, Evensen G, Drange H, Jenkins AD. 1999. Coordinate Transformation on a Sphere Using Conformal Mapping. Monthly Weather Review 127:2733-2740.

Broms C, Melle W. 2007. Seasonal development of Calanus finmarchicus in relation to phytoplankton bloom dynamics in the Norwegian Sea. Deep Sea Research Part II: Topical Studies in Oceanography 54:2760-2775.

Broms C, Melle W, Kaartvedt S. 2009. Oceanic distribution and life cycle of Calanus species in the Norwegian Sea and adjacent waters. Deep Sea Research Part II: Topical Studies in Oceanography 56:1910-1921.

Bryant AD, Hainbucher D, Heath M. 1998. Basin-scale advection and population persistence of *Calanus finmarchicus*. Fisheries Oceanography 7:235-244.

Budgell W. 2005. Numerical simulation of ice-ocean variability in the Barents Sea

region. Ocean Dynamics 55:370-387.

Carlotti F, Giske J, Werner F. 2000. Modeling zooplankton dynamics. in: Harris R., Wiebe P., Lenz J., Skjoldal H. R. and Huntley M., editor. ICES zooplankton methodology manual. Academic Press. p 571-667.

Carlotti F, Krause M, Radach G. 1993. Growth and development of *Calanus finmarchicus* related to the influence of temperature: experimental results and conceptual model. Limnology and Oceanography 38:1125-1134.

Carlotti F, Nival P. 1992. Model of copepod growth and development: moulting and mortality in relation to physiological processes during an individual moult cycle. Marine Ecology Progress Series 84:219-233.

Carlotti F, Radach G. 1996. Seasonal dynamics of phytoplankton and *Calanus finmarchicus* in the North Sea as revealed by a coupled one-dimensional model. Limnology and Oceanography 41:522-539.

Carlotti F, Wolf KU. 1998. A Lagrangian ensemble model of *Calanus finmarchicus* coupled with a 1-D ecosystem model. Fisheries Oceanography 7:191-204.

Chambers CR. 1993. Phenotypic variability in fish populations and its representation in individual-based models. Transactions of the American Fisheries Society 122:404-414.

Dale T, Bagoien E, Melle W, Kaartvedt S. 1999. Can predator avoidance explain varying overwintering depth of Calanus in different oceanic water masses? Marine Ecology Progress Series 179:113- 121.

Dalpadado P, Ellertsen B, Melle W, Dommasnes A. 2000. Food and feeding conditions of Norwegian spring-spawning herring (Clupea harengus) through its feeding migrations. ICES Journal of Marine Science 57:843-857.

Dalpadado P, Ellertsen B, Melle W, Skjoldal HR. 1998. Summer distribution patterns and biomass estimates of macrozooplankton and micronekton in the Nordic Seas. Sarsia 83:103-116.

Dommasnes A, Melle W, Dalpadado P, Ellertsen B. 2004. Herring as a major consumer in the Norwegian Sea. ICES Journal of Marine Science 61:739-751.

Ellertsen B, Melle W. 2009. Section 2.3.2 Sekundærproduksjon (Dyreplankton)-Zooplankton. In: Fisken og havet (særnummer 1-2009) Havets ressurser og miljø. Institute of Marine Research, Bergen, Norway, p 74-76.

EMEP/MSC-W. 1998. Transboundary acidifying air pollution in Europe. EMEP/MSC-W Report 1/98, The Norwegian Meteorological Institute (http://emep.int/publ/reports/1998/EMEP_1998_R1_p2.pdf).

Falkowski PG, Ziemann D, Kolber Z, Bienfang PK. 1991. Role of eddy pumping in enhancing primary production in the ocean. Nature 352:55-58.

Fiksen Ø. 2000. The adaptive timing of diapause - a search for evolutionarily robust strategies in *Calanus finmarchicus*. ICES Journal of Marine Science 57:1825-1833.

Gehlen M, Malschaert H, Van Raaphorst WR. 1995. Spatial and temporal variability of benthic silica fluxes in the southeastern North Sea. Continental Shelf Research 15:1675-1696.

Gentleman WC, Neuheimer AB, Campbell RG. 2008. Modelling copepod development: current limitations and a new realistic approach. ICES Journal of Marine Science: Journal du Conseil 65:399-413.

Godø OR, Patel R, Samuelsen A, Hjøllo SS, Horne J, Anderson CIH, Hansen C, Bertino L, Kaartvedt S, Johannessen JA. In prep. Mesoscale eddies create productive habitats for higher trophic marin life.

Grimm V, Railsback SF. 2005. Individual-based modeling and ecology. Princeton and Oxford: Princeton University Press. 428 pages.

Haidvogel DB, Arango HG, Hedstrom K, Beckmann A, Malanotte-Rizzoli P, Shchepetkin AF. 2000. Model evaluation experiments in the North Atlantic Basin: simulations in nonlinear terrainfollowing coordinates. Dynamics Of

Atmospheres And Oceans 32:239-281.

Haidvogel DB, Beckmann A. 1999. Numerical Ocean Circulation Modeling. London: Imperial College Press. 318 pages.

Hansen C, Samuelsen A. 2009. Influence of horizontal model grid resolution on the simulated primary production in an embedded primary production model in the Norwegian Sea. Journal of Marine Systems 75:236-244.

Heath MR, Backhaus JO, Richardson K, McKenzie E, Slagstad D, Beare D, Dunn J, Fraser JG, Gallego A, Hainbucher D, Hay S, Jonasdottir S, Madden H, Mardaljevic J, Schacht A. 1999. Climate fluctuations and the spring invasion of the North Sea by Calanus finmarchicus. Fisheries Oceanography 8:163-176.

Hirche HJ. 1996a. Diapause in the marine copepod, *Calanus finmarchicus* - a review. Ophelia 44:129- 143.

Hirche HJ. 1996b. The reproductive biology of the marine copepod, *Calanus finmarchicus* - a review. Ophelia 44:111-128.

Hirche HJ, Brey T, Niehoff B. 2001. A high-frequency time series at ocean Weather ship station M (Norwegian Sea): population dynamics of Calanus finmarchicus. Marine Ecology Progress Series 219:205-219.

Hunke EC. 2001. Viscous-Plastic Sea Ice Dynamics with the EVP Model: Linearization Issues. Journal of Computational Physics 170:18-38.

Hunke EC, Dukowicz JK. 1997. An Elastic-Viscous-Plastic Model for Sea Ice Dynamics. Journal of Physical Oceanography 27:1849-1867.

Huse G. 2005. Artificial evolution of *Calanus* life history strategies under different predation levels. Globec International Newsletter 11:19.

Huse G, Giske J, Salvanes AGV. 2002. Individual-based models. in: Hart P. J. B. and Reynolds J., editor. Handbook of Fish and Fisheries. Oxford: Blackwell Science. p 228-248.

Huse G, Melle W, Skogen M, Svendsen E, Budgell P. in prep. A 3D super-individual model with emergent life history and behaviour for *Calanus finmarchicus* in the Norwegian Sea Huse G, Strand E, Giske J. 1999. Implementing behaviour in individual-based models using neural networks and genetic algorithms. Evolutionary Ecology 13:469-483.

Huston M, DeAngelis D, Post W. 1988. New computer models unify ecological theory. BioScience 38:682-691.

Kalnay E, Kanamitsu M, Kistler R, Collins W, Deaven D, Gandin L, Iredell M, Saha S, White G, Woollen J, Zhu Y, Chelliah M, Ebisuzaki W, Higgins W, Janowiak J, Mo KC, C. R, Wang J, Leetmaa A, Reynolds R, Jenne R, Joseph D. 1996. The NCEP/NCAR 40-year reanalysis project. Bulletin of the American Meteorological Society 77:437-471.

Langøy H, Nøttestad L, Skaret G, Broms C, Fernö A. this issue. Overlap in distribution and diets of Atlantic mackerel (Scomber scombrus), Norwegian spring-spawning herring (Clupea harengus) and blue whiting (Micromesistius poutassou) in the Norwegian Sea during late summer. Marine Biology Research

Large WG, Gent PR. 1999. Validation of Vertical Mixing in an Equatorial Ocean Model Using Large Eddy Simulations and Observations. Journal of Physical Oceanography 29:449-464.

Lien VS, P. B, Ådlandsvik B, Svendsen E. 2006. Validating results from the model ROMS, with respect to volume transports and heat fluxes in the Nordic Seas. Technical Report Fisken og Havet 2/2006.Institute of Marine Research, Bergen, Norway. 58 pages.

Lohse L, Kloosterhuis H, van Raaphorst W, Helder W. 1996. Denitrification rates as measured by the isotope pairing method and by the acetylene inhibition technique in continental shelf sediments of the North Sea. Marine Ecology Progress Series 132:169-179.

Lohse L, Malschaert F, Slomp C, Helder W, Raaphorst W. 1995. Sediment–water fluxes of inorganic nitrogen compounds along the transport route of organic matter in the North Sea. Ophelia 41 41:173-197.

Marshall SM, Orr AP. 1955. The biology of a marine copepod . Edinburgh & London: Oliver & Boyd. 188 pages.

Mayer B. 1995. Ein dreidimensionales numerisches Schwebstoff-Transportmodell mit Anwendung auf die Deutsche Bucht. Dissertation im Fachbereich Geowissenschaften der Universität Hamburg. Report no GKSS--95/E/59. 104 pages.

Melle V, Ellertsen B, Skjoldal HR. 2004. Zooplankton: The link to higher trophic levels. in: Skjoldal H. R., editor. The Norwegian Sea Ecosystem. Trondheim: Tapir Academic Press. p 137-202.

Munk P, Hansen BW, Nielsen TG, Thomsen HA. 2003. Changes in plankton and fish larvae communities across hydrographic fronts off West Greenland. Journal of Plankton Research 25:815-830.

Nash RDM, Dickey-Collas M. 2005. The influence of life history dynamics and environment on the determination of year class strength in North Sea herring (*Clupea harengus* L.). Fisheries Oceanography 14:279-291.

Niehoff B, Klenke U, Hirche HJ, Irigoien X, Head R, Harris R. 1999. A high frequency time series at Weathership M, Norwegian Sea, during the 1997 spring bloom: the reproductive biology of Calanus finmarchicus. Marine Ecology Progress Series 176:81-92.

Ohman MD, Eiane K, Durbin EG, Runge JA, Hirche HJ. 2004. A comparative study of Calanus finmarchicus mortality patterns at five localities in the North Atlantic. ICES Journal of Marine Science 61:687-697.

Oki T, Sud YC. 1998. Design of Total Runoff Integrating Pathways (TRIP) - A Global River Channel Network. Earth Interactions 2:1-37.

Payne MR, Hatfield EMC, Dickey-Collas M, Falkenhaug T, Gallego A, Groger J, Licandro P, Llope M, Munk P, Rockmann C, Schmidt JO, Nash RDM. 2009. Recruitment in a changing environment: the 2000s North Sea herring recruitment failure. ICES Journal of Marine Science 66:272-277

Pedersen OP, Tande KS, Slagstad D. 2001. A model study of demography and spatial distribution of Calanus finmarchicus at the Norwegian coast. Deep-Sea Research Part II-Topical Studies in Oceanography 48:567-587.

Planque B, Fromentin JM. 1996. Calanus and environment in the eastern North Atlantic .1. Spatial and temporal patterns of C-finmarchicus and C-helgolandicus. Marine Ecology Progress Series 134:101-109.

Pohlmann T, Puls W. 1994. Currents and transport in water. in: Sündermann J., editor. Circulation and Contaminant Fluxes in the North Sea. Section 3.2. Berlin: Springer. p 345-402.

Reid PC, Edwards M, Beaugrand G, Skogen M, Stevens D. 2003. Periodic changes in the zooplankton of the North Sea during the twentieth century linked to oceanic inflow. Fisheries Oceanography 12:260-269.

Rey F. 2004. Phytoplankton: the grass of the sea. in: Skjoldal H. R., editor. The Norwegian Sea ecosystem. Tapir Academic Press. p 97-136.

Samuelsen A, Huse G, Hansen C. 2009. Shelf recruitment of *Calanus finmarchicus* off the west coast of Norway: role of physical processes and timing of diapause termination. Marine Ecology Progress Series 386:163-180.

Scheffer M, Baveco JM, DeAngelis DL, Rose KA, van Nes EH. 1995. Super-individuals a simple solution for modelling large populations on an individual basis. Ecological Modelling 80:161- 170.

Shchepetkin AF, McWilliams JC. 2003. A method for computing horizontal pressure-gradient force in an oceanic model with a nonaligned vertical coordinate. Journal of Geophysical Research (C3)- 108:3090-3124.

Shchepetkin AF, McWilliams JC. 2005. The regional oceanic modeling system

(ROMS): a split-explicit, free-surface, topography-following-coordinate oceanic model. Ocean Modelling 9:347-404.

Skartveit A, Olseth JA. 1986. Modelling slope irradiance at high latitudes. Solar Energy 36:333-344.

Skartveit A, Olseth JA. 1987. A model for the diffuse fraction of hourly global radiation. Solar Energy 38:271-274.

Skjoldal HR, Dalpadado P, Dommasnes A. 2004a. Food webs and trophic interactions. in: Skjoldal H. R., editor. The Norwegian Sea ecosystem. Trondheim: Tapir Academic Press. p 447-506. Skjoldal HR, Sætre R, Fernö A, Misund OA, Røttingen I. 2004b. The Norwegian Sea Ecosystem. Trondheim: Tapir Academic Press. 559 pages.

Skogen M, Søiland H. 1998. A user guide to NORWECOM v2.0, The Norwegian Ecological Model System. Fisken og Havet No 18, Institute of Marine Research. :42p.

Skogen MD, Budgell WP, Rey F. 2007. Interannual variability in Nordic seas primary production. ICES Journal of Marine Science 64:889-898.

Skogen MD, Svendsen E, Berntsen J, Aksnes D, Ulvestad KB. 1995. Modelling the primary production in the North Sea using a coupled three-dimensional physical-chemical-biological ocean model. Estuarine, Coastal and Shelf Science 41:545-565.

Skogen MD, Svendsen E, Ostrowski M. 1997. Quantifying volume transports during SKAGEX with the Norwegian Ecological Model system. Continental Shelf Research 17:1817-1837.

Skogen MD, Søiland H, Svendsen E. 2004. Effects of changing nutrient loads to the North Sea. Journal of Marine Systems 46:23-38.

Song YH, Haidvogel D. 1994. A Semiimplicit Ocean Circulation Model Using a Generalized Topography-Following Coordinate System. Journal of Computational Physics 115:228-244.

Speirs DC, Gurney WSC, Heath MR, Horbelt W, Wood SN, de Cuevas BA. 2006. Ocean-scale modeling of the distribution, abundance, and seasonal dynamics of the copepod *Calanus finmarchicus*. Marine Ecology Progress Series 313:173-192.

Speirs DC, Gurney WSC, Heath MR, Wood SN. 2005. Modelling the basin-scale demography of Calanus finmarchicus in the north-east Atlantic. Fisheries Oceanography 14:333-358.

Stenevik EK, Melle W, Gaard E, Gislason A, Broms CTÅ, Prokopchuk I, Ellertsen B. 2009. Egg production of Calanus finmarchicus--A basin-scale study. Deep Sea Research Part II: Topical Studies in Oceanography 54:2672-2685.

Sætersdal G, Loeng H. 1987. Ecological adaptation of reproduction in Northeast Arctic Cod. Fisheries Research 5:253-270.

Søiland H, Skogen MD. 2000. Validation of a three-dimensional biophysical model using nutrient observations in the North Sea. ICES Journal of Marine Sciences 57:816-823.

Tittensor DP, Deyoung B, Tang CL. 2003. Modelling the distribution, sustainability and diapause emergence timing of the copepod *Calanus finmarchicus* in the Labrador Sea. Fisheries Oceanography 12:299-316.

Utne KR, Hjøllo SS, Huse G, Skogen M. this issue. Total consumption of *Calanus finmarchicus* by planktivorous fish in the Norwegian Sea estimated from a fully coupled model system. Marine Biology Research

1
2
3
4
5
6
7
8
9
10
11
12
13
14
15
16
17
18
19
20
21
22
23
24
25
26
27
28
29
30
31
32
33
34
35
36
37
38
39
40
41
42
43
44
45
46
47
48
49
50
51
52
53
54
55
56
57
58
59
60

Table 1 **The strategy and attribute vectors of individuals in the initial field.**

| Element | Category | Initial value |
|---------|----------|---------------|
| Overwintering depth | SV | 300-1100 m |
| Wake up day | SV | Day 70 ± 30 days |
| Allocation to fat day | SV | WUD + 60 ± 30 days |
| Fat/soma ratio | SV | 0.4 ± 0.2 |
| VM1 | SV | not used |
| VM2 | SV | not used |
| Stage | AV | C5 |
| Internal number | AV | $0\text{-}6\cdot10^{14}$ |
| Structural weight | AV | 40µgC |
| Fat level | AV | 8 KJ |
| Position | AV | Within Nordic Seas |
| Depth | AV | 0-1300m |
| Moult cycle fraction | AV | 0 |
| Total no of eggs | AV | 0 |

Table 2 **Overview of experiments**

| Exp no | Wake Up Day | Allocation to Fat Day | Comments |
|--------|-------------|------------------------|----------|
| REFRUN | Feb10 - April 9 | Mar 9- July 10 | Reference run |
| WUDEARLY | Jan 28 – Mar 21 | Feb 20 – Jun 20 | WUD early |
| WUDLATE | Feb 20 – Apr 20 | Mar 20 – Jul 20 | WUD late |
| WUDLIGHT | Feb 10 – Mar 24 | Mar 9 – Jun 28 | WUD daylight dependent |
| NOFLA | Feb10 - April 9 | Mar 9- July 10 | Access to diatoms only |
| LOWINI | Feb10 - April 9 | Mar 9- July 10 | Initial biomass 4.4 mill tonnes C |

Figure 1 Bottom topography in the Norwegian Sea and adjacent areas. Contour lines area drawn for 100, 500, 1000, 2000 and 3000 meters, respectively. M denotes position of Ocean Weather Ship M and squares represent position where *Calanus finmarchicus* observations for 1997 (presented in figure 6) are taken. Blue squares represent positions where *both* abundance and biomass estimates are available, black squares represent positions for observed biomass only.

**Deleted:** .

Figure 2. Left side: Daily values of biomass, production, number of individuals and number of super-individuals for experiments starting with uniform biomass distribution and then evolved for 4 years. Right side: abundance at day 1 in the 4 years.

Figure 3 Left side: Anomalies (fraction of parameter-value in the run with 200.000 individuals) in daily values of biomass, accumulated production and number of individuals for experiments combing super-individuals within the same or adjacent square, and with mean fat/structural weight within 5-20%. Right side: abundance at day 1 for the same experiments.

Figure 4 Left side: Daily values of biomass, production, number of individuals and number of super-individuals for the reference run. Right side: abundance at day 1 in January (only C5), May (C1-C6 and only C6) and December (only C5) for the reference run. Note that lower left panel is a close up of the southern Norwegian Sea and that the values are multiplied by 10 to fit the color scale.

Figure 5 a) Upper 200m *Calanus* abundance at OWSM(66˚N,2˚E), from observations and model for the year 1997. Data are sorted by stage C1-C6, and are grouped into monthly values. Vertical lines indicate 95% confidence interval. b) Chlorophyll-a observed (stippled line) and modeled (full line), and modeled from an earlier uncoupled simulation by (thin line). Observations from Rey (2004), uncoupled simulation from Skogen et al. (2007).

Figure 6 Upper 200m *Calanus* abundance (upper) and biomass (lower) at locations shown in Figure 1, from observations and model for the year 1997. Model values are picked at same time and location as observations are available. Observed biomass is estimated assuming 50% and 70% *Calanus* content (predominantly *C. finmarchicus)* in the size classes <1000µm and 1000-2000µm respectively, as suggested by Skjoldal et al (2004a). Modeled biomass is C1-C6 *C. finmarchicus* biomass transformed from carbon to dry weight using a converting factor of 2. (Hirche et al. 2001a). Vertical lines indicate 95% confidence interval.

Figure 7. Daily values of biomass and production in reference run and six different experiments.

Figure 8. Daily values of the population's mean wake-up-day (upper panel) and allocation-to-fat-day (lower panel) for the reference run and additional experiments.

Figure 1
152x114mm (300 x 300 DPI)

Figure 2a
152x114mm (300 x 300 DPI)

Figure 2b
152x114mm (300 x 300 DPI)

Fig3a
152x114mm (300 x 300 DPI)

Abundance

200.000

120.000

47.000

23.000

[1000 ind/m$^2$]

100　　200　　300
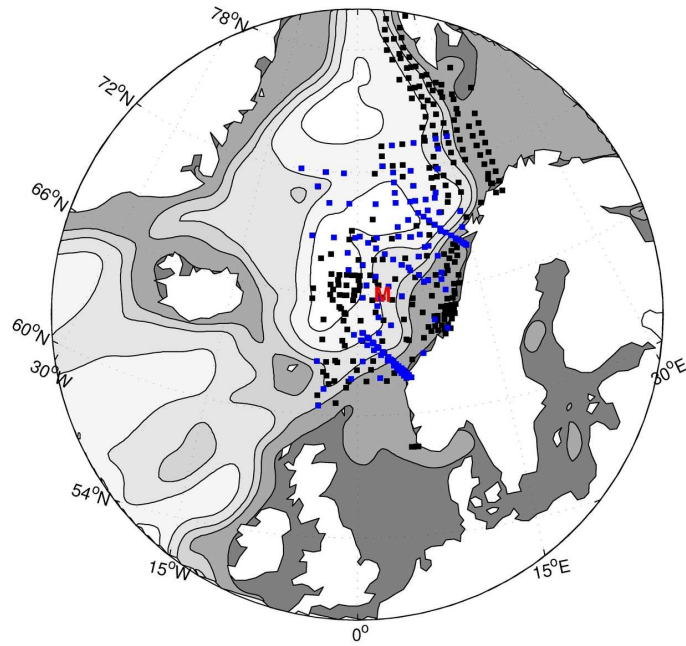
Fig3b
152x114mm (300 x 300 DPI)

1
2
3
4
5
6
7
8
9
10
11
12
13
14
15
16
17
18
19
20
21
22
23
24
25
26
27
28
29
30
31
32
33
34
35
36
37
38
39
40
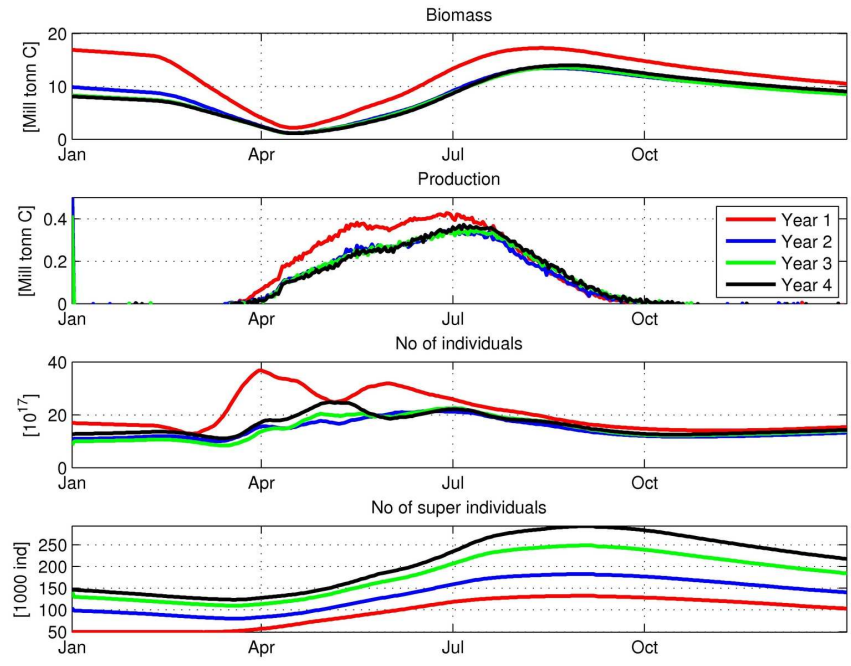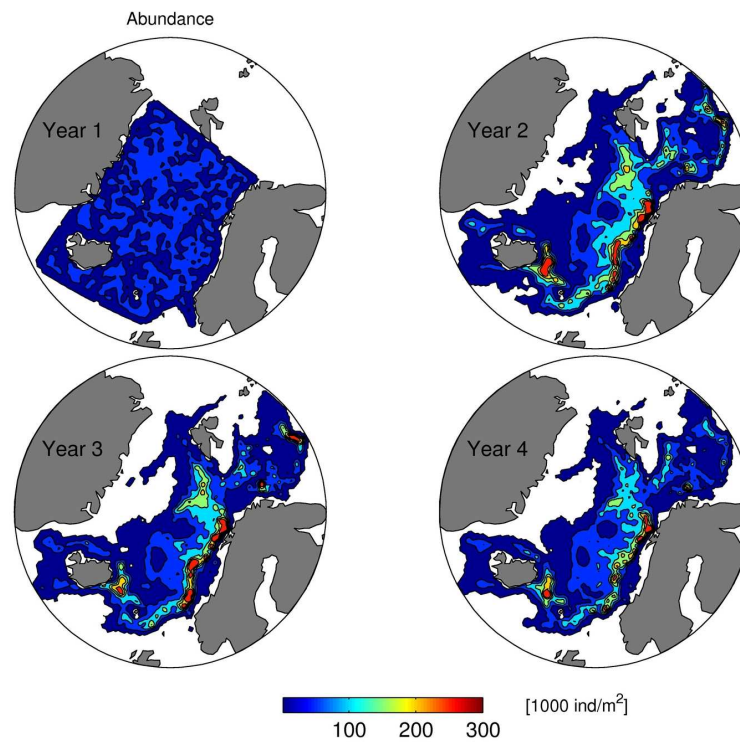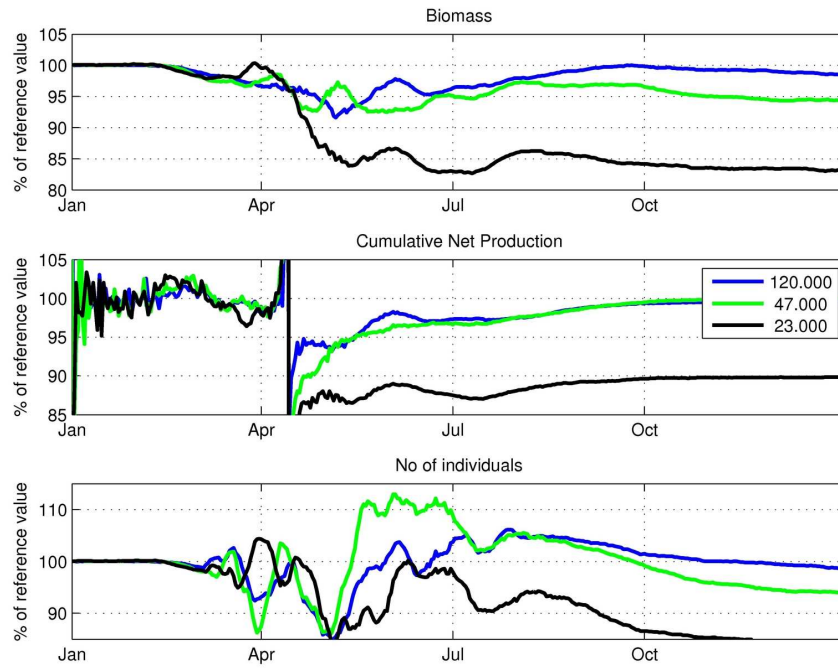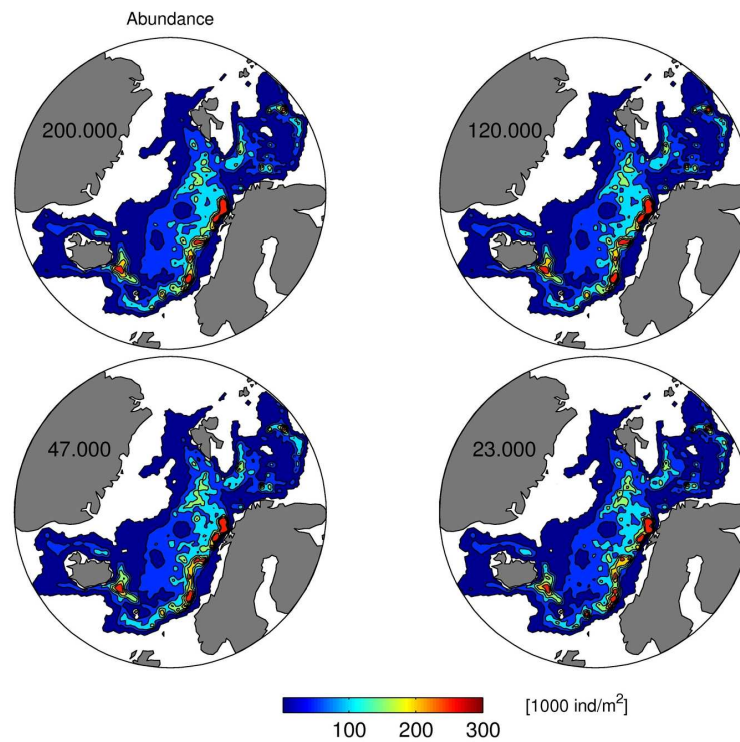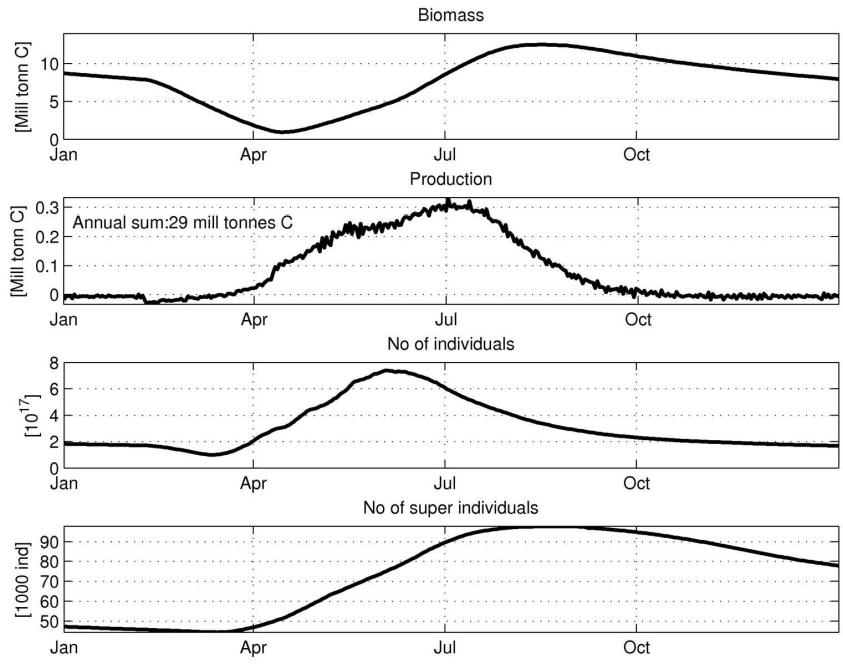41
42
43
44
45
46
47
48
49
50
51
52
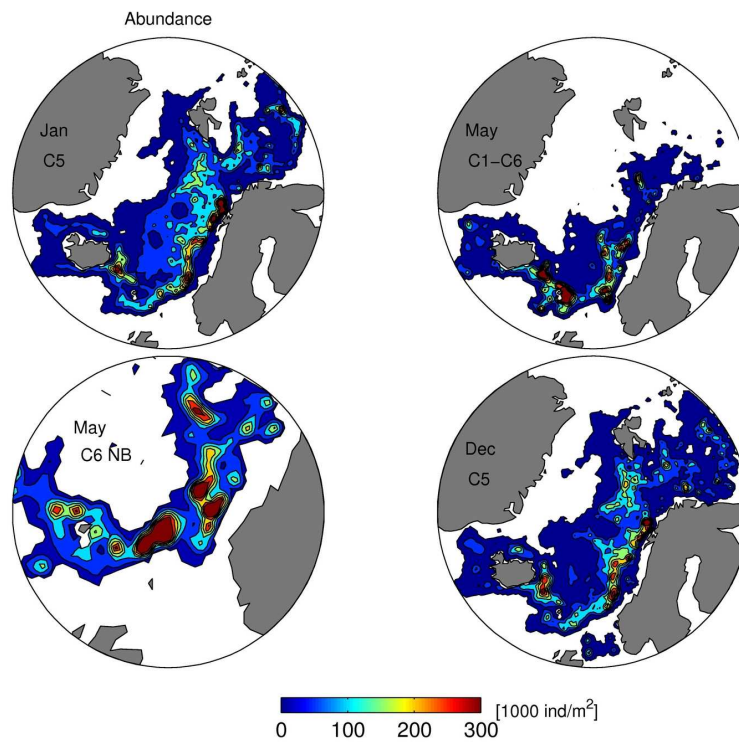53
54
55
56
57
58
59
60
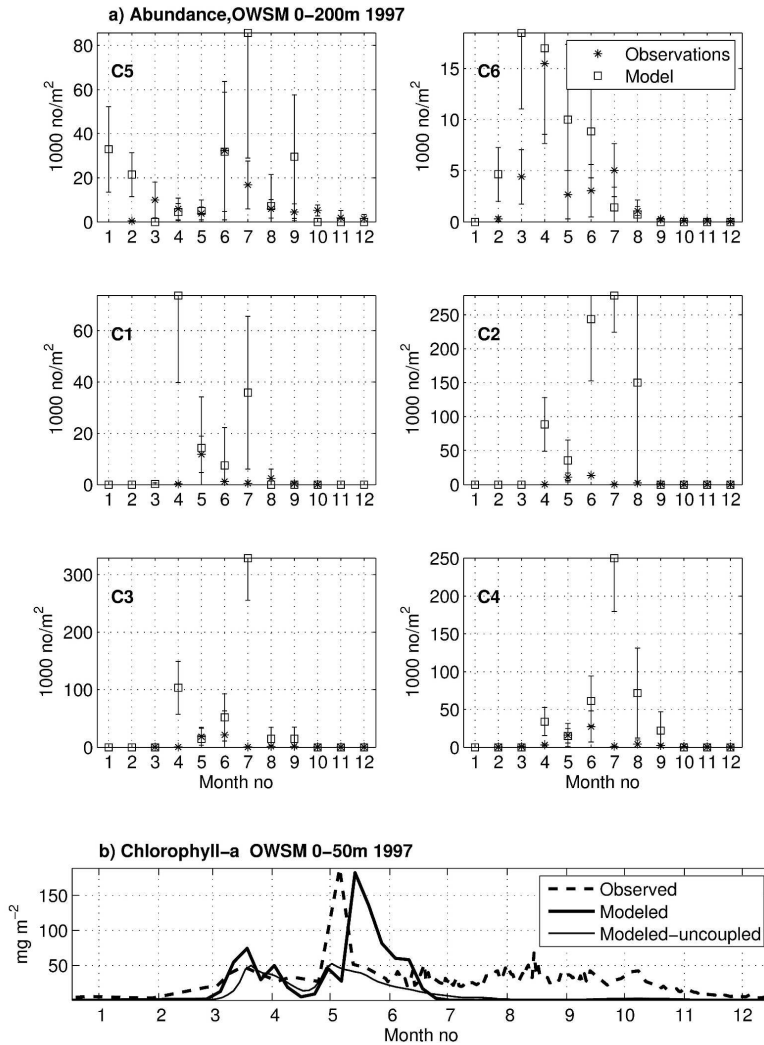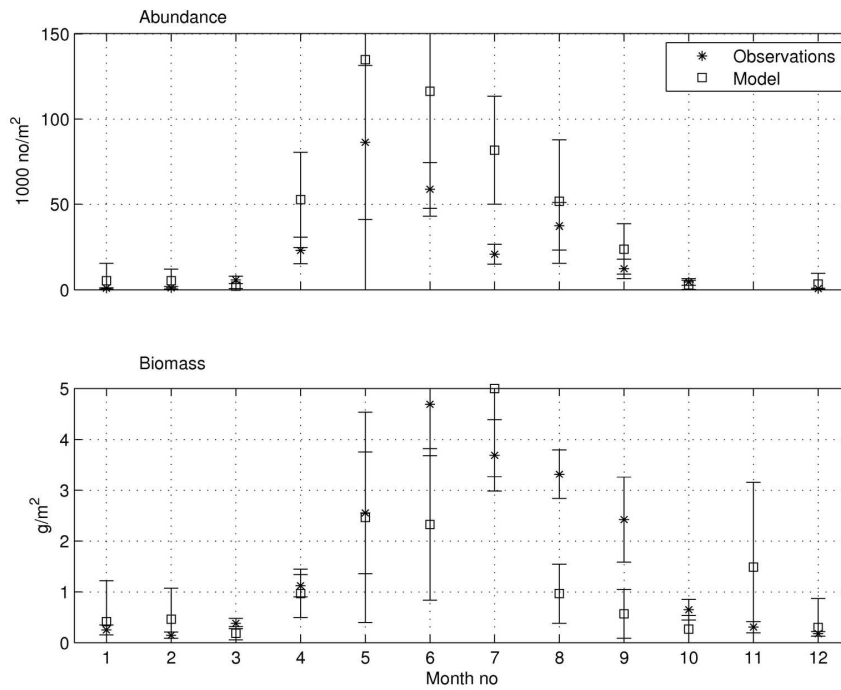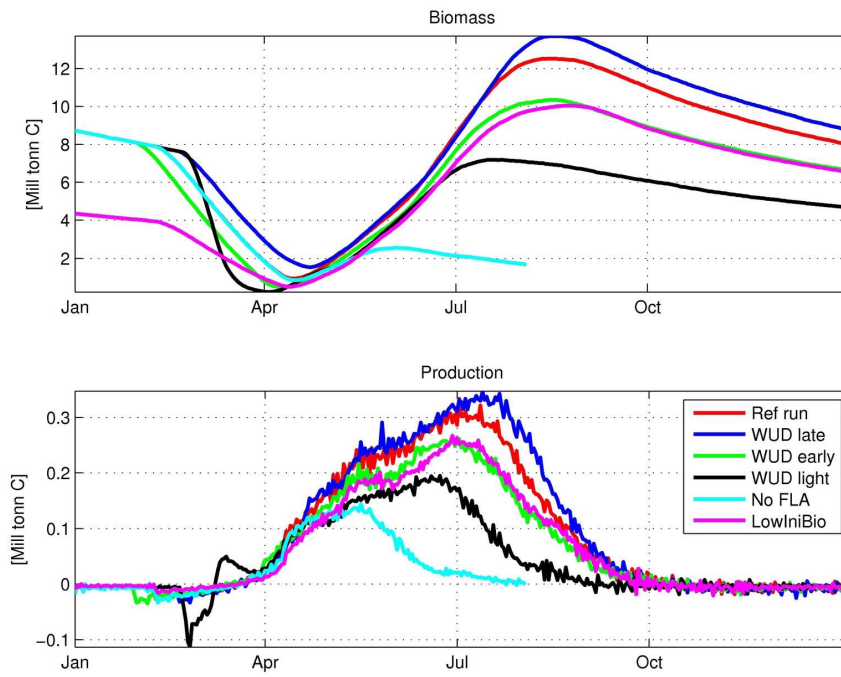
Fig4a
152x114mm (300 x 300 DPI)
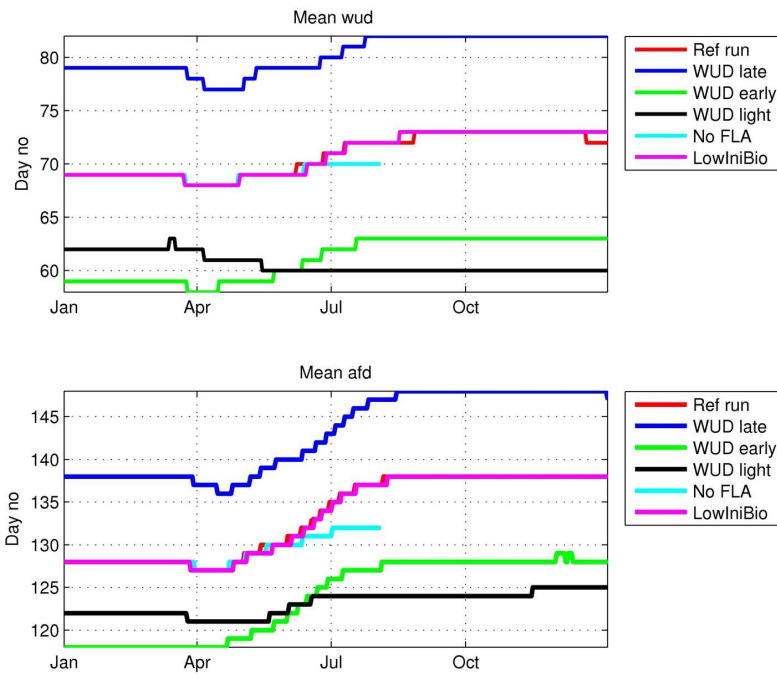
Fig4b
152x114mm (300 x 300 DPI)

1
2
3
4
5
6
7
8
9
10
11
12
13
14
15
16
17
18
19
20
21
22
23
24
25
26
27
28
29
30
31
32
33
34
35
36
37
38
39
40
41
42
43
44
45
46
47
48
49
50
51
52
53
54
55
56
57
58
59
60



Fig5
284x410mm (300 x 300 DPI)

Fig6
152x114mm (300 x 300 DPI)

Figure 7
152x114mm (300 x 300 DPI)

Figure 8
152x114mm (300 x 300 DPI)